Functionalization of Acyclic Xeno Nucleic Acid with Modified Nucleobases

Keiji Murayama, Yuuhei Yamano, Hiroyuki Asanuma

Abstract

Xeno nucleic acids (XNAs), which are composed of artificial scaffolds and natural nucleobases, have unique hybridization properties that depend on the scaffold structure. Here, we functionalized the acyclic XNA, serinol nucleic acid (SNA), with non-natural nucleobases. A linear SNA probe functionalized with 5-perylenylethynyl uracil residues showed weak greenish-yellow excimer emission in the absence of target RNA and bright cyan-green monomer emission in the presence target RNA. Probe hybridization was rapid and enabled quantitative detection of RNA with discrimination of single-base mismatch. We also designed a photo-responsive SNA with two 8-pyrenylvinyl adenine (^{PV}A) residues. Irradiation with blue (455 nm) light caused [2+2] photocycloaddition between intrastrand ^{PV}As, resulting in dissociation of an SNA/RNA duplex, whereas irradiation with ultraviolet (340 nm) light induced cyclo-reversion of the ^{PV}A photo-dimer and SNA/RNA duplex reformation. Using a combination of 8-naphthylvinyl adenine (^{NV}A) and ^{PV}A and irradiation with 465 nm, 405 nm, 340 nm, and 300 nm light, orthogonal control of formation of SNA(^{NV}A-^{NV}A)/RNA and SNA(^{PV}A-^{NV}A)/RNA duplexes was demonstrated. Thus, modifications of nucleobases further expand the utility of acyclic XNA in bio-nanotechnology.

Introduction

Phosphoramidite chemistry allows facile synthesis of natural nucleic acids as well as oligomers containing various unnatural monomers.[1] By using this technology, xeno nucleic acids (XNAs), which are DNA analogues, have been developed to improve performance of nucleic acid-based biological tools and to understand why nature selected D-ribose as a scaffold of genetic carrier.[2–8] XNAs are resistant to digestion by exo- and endonucleases, enabling use of XNAs in a variety of biological applications including as fluorescent probes,[9–11] antisense reagents,[12–15] small interfering RNAs (siRNAs),[16–19] and other functional biological tools.[20–22] XNAs with cyclic backbone structures have been widely investigated because the rigid cyclic backbone stabilizes duplexes by pre-organization for hybridization. In some case, XNAs with cyclic backbones are compatible with enzymatic reactions due to similarities to the structure of DNA.[20–23] Our group has focused on development of acyclic XNAs including acyclic threoninol nucleic acid (*a*TNA) derivatives (D-*a*TNA[24], L-*a*TNA[25], *allo*-*a*TNA[26]) and serinol nucleic acid (SNA),[27] which are composed of aminodiol scaffolds (Fig. 1A).

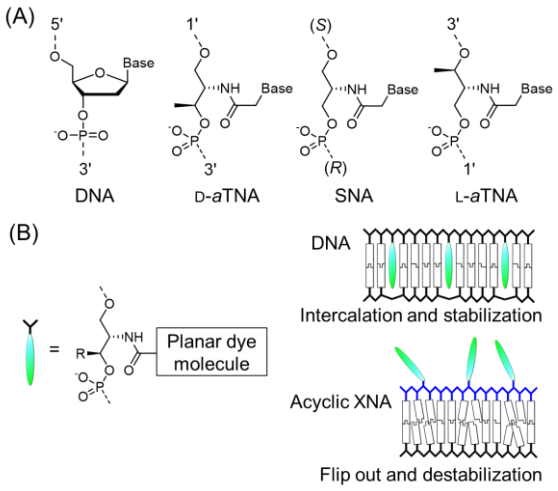

Figure 1. (A) Chemical structures of DNA and acyclic XNAs. (B) Illustration of differences in duplex structures when planar dye molecules are incorporated into DNA and acyclic XNA strands.

Complementary oligomers of D-*a*TNA, L-*a*TNA, and SNA form highly stable homo-duplexes. L-*a*TNA, which forms a right-handed homo-duplex, hybridizes with complementary D-DNA and D-RNA, whereas D-*a*TNA, which has left-handed helical preference in the homo-duplex, cannot recognize natural nucleic acids with D-ribose. SNA cross-hybridizes with D-DNA, L-DNA, D-RNA and L-RNA as well as chiral XNAs with right-handed and left-handed helical preferences in duplex state.[7,8] Because of these properties, acyclic XNAs are applicable to novel biological tools.[28,29] However, with only natural four nucleobases, functions of XNAs are limited. Previously, our group has functionalized DNA with additional insertion of base surrogates;[30,31] however, this methodology cannot be used for functionalization of acyclic XNAs because the base surrogates do not intercalate probably due to strong stacking between base pairs (Fig. 1B). For acyclic XNAs, nucleobase modification rather than insertion of base surrogates is necessary. Since modification of nucleobases on acyclic XNAs is synthetically straightforward, modified nucleobases that are stimulus-responsive,[32–40] that have fluorescent properties,[41–46] or that serve to expand the genetic code[47–52] can be used to functionalize XNA. In this focus review, we describe fluorescent probes and photo-responsive systems composed of acyclic XNAs.

Fluorescent probe composed of SNA modified with 5-perylenylethynyl uracil (^{Pe}U)

Fluorescent probes are used to image RNA in cells and in clinical biopsies.[53,54] Such probes must be stable in the presence of enzymes that degrade nucleic acids and must have affinity and specificity for the target RNA. Although DNA-based probes are widely used, digestion by nucleases and relatively low affinity with target RNA are problematic. We have successfully developed a molecular beacon composed of SNA that can detect RNA with extremely high sensitivity.[28] SNA beacon has several advantages over DNA including durability in the presence of nucleases, low background emission, and high affinity for RNA. However, a molecular beacon can tether only single pair of dyes, limiting brightness. We therefore recently designed a light-up type SNA linear probe containing multiple fluorescent dyes, which detects complementary DNA and RNA with high brightness, based on a DNA linear probe. The DNA linear probe tethering multiple perylenes via D-threoninol caused weak interaction among the perylenes allows self-quenching of the fluorophores in the single-stranded state, whereas the fluorophores intercalate and recover fluorescence upon hybridization with the target strand.[55]

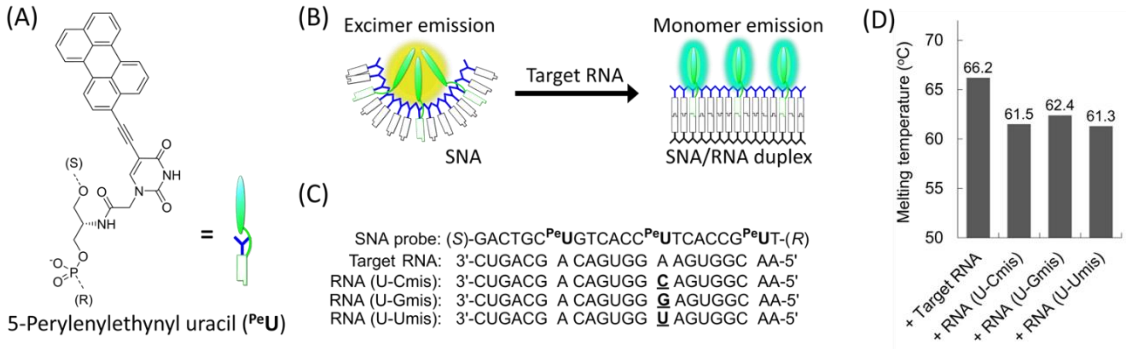

Figure 2. A) Chemical structure of an SNA backbone conjugated to ^{Pe}U. B) Design of SNA linear probe with multiple ^{Pe}U residues. C) Sequences of probe SNA, target RNA, and mismatched RNA. Underline indicates mismatched base. D) Melting temperatures of duplexes of SNA probe with target RNA and mismatched RNAs. The solution conditions were 100 mM NaCl, 10 mM phosphate buffer (pH 7.0), 2.0 μM oligomer. Adapted with permission from ref. 56 with partial modifications. (Copyright 2020)

To avoid destabilization of the duplex by the incorporation of dyes into SNA, we incorporated three fluorescent nucleobase analogues into the SNA strand.[56] The analogue ^{Pe}U (Fig. 2A)[44] was selected because association of perylenes induces excimer emission at a wavelength that is discriminable from monomer emission and because the rigid ethynyl linker was predicted to limit association of perylenes in the duplex state. In the single strand, the flexible acyclic serinol scaffold should allow aggregation of perylene moieties facilitating excimer emission, whereas in the presence of the target RNA, the chromophores rigidly linked to ^{Pe}U should be separated, resulting in bright monomer emission (Fig. 2B). A 22-mer RNA sequence was selected as a model target and the complementary SNA linear probe tethering

three ^{Pe}U residues, each separated by six nucleobases, was designed (Fig. 2C). ^{Pe}U was incorporated into SNA via conventional phosphoramidite chemistry. The SNA probe hybridized with target RNA with a high melting temperature (T_m) of 66.2 °C. In contrast, when the RNA contained a single mismatch to the probe, duplexes were less stable with T_ms lower by 3.8 to 4.9 °C (Fig. 2D). This result indicated that pairing between ^{Pe}U and adenine occurred selectively.

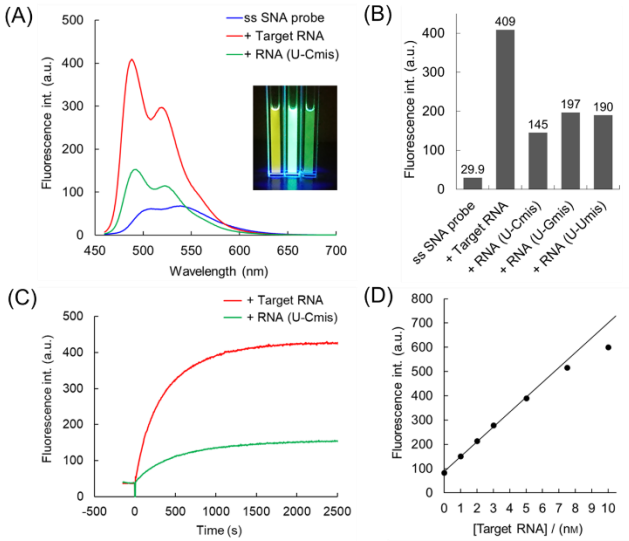

Figure 3. A) Fluorescence spectra of single-stranded SNA and of SNA/RNA duplexes at 40 °C. Conditions: 0.5 μM SNA, 1.0 μM RNA, 100 mM NaCl, 10 mM phosphate buffer (pH 7.0), ex. = 450 nm. Insert: Cells containing single-stranded SNA (left), SNA and target RNA (center), and SNA and mismatched RNA (U-Cmis) (right) irradiated with 450 nm light and photographed through a high pass optical filter (480 nm). B) Fluorescence intensities of SNA alone (ssSNA) or with target RNA or mismatched RNAs. C) Changes in fluorescence intensity of SNA probe with time by the addition of target RNA (red line) or U-Cmis (green line). Target was added at 0 s. Conditions: ex. = 450 nm, em. = 488 nm, 50 nM SNA, 100 nM RNA, 100 mM NaCl, 10 mM phosphate buffer (pH 7.0), 37°C D) Plot of emission intensity of 10 nM SNA probe at 488 nm vs. concentration of target RNA. The samples were incubated at 45°C for 1 h after each addition of RNA to ensure that equilibrium was reached. Adapted with permission from ref. 56 with partial modifications. (Copyright 2020)

In the solution of the single-stranded SNA probe, monomer emission was quenched, whereas excimer emission appeared at 500~600 nm (Fig. 3A, blue line). Upon duplex formation with target RNA, a bright monomer emission with peak maximum at 488 nm was detected (Fig. 3A, red line). The ratio of intensity at 488 nm in the presence of the target to that in the absence of the target was 13.7 in aqueous buffer at 40 °C (Fig. 3B). The emission intensities were considerably reduced in the solution of the SNA probe with RNA containing a single mismatched nucleobase (Fig. 3A, green line). The differences in fluorescent behaviors were detectable with the naked eye (Fig. 3A, insert). The mismatched base pair presumably distorted the duplex structure, resulting in the quenching of fluorescence emission via intra-strand contact of perylene moieties. Analysis of emission as a function of time revealed that the emission intensity increased immediately and reached a plateau at 1500 s after addition of the full-matched target RNA to the SNA probe (Fig. 3C, red line). In the case of mismatched RNA, the hybridization kinetics did not differ, but the intensity at the plateau was about one-third that in the presence of fully matched target RNA (Fig. 3C, green line). At least 1.0 nM (0.1 eq.) target RNA was detectable, and the SNA probe quantitatively detected target RNA with a linear change in emission intensity in the range of 1.0 to 5.0 nM target (Fig. 3D).

These experiments demonstrated that the quencher-free SNA probe carrying ^{Pe}U residues selectively hybridized with target RNA as detectable by a change in fluorescent behavior between monomer emission and excimer emission. This probe successfully discriminated a fully matched target RNA from an RNA with a single-base mismatch. The rapid response, quantitative detection, and high durability against nucleases mean that SNA linear probes should prove useful for detection and imaging of RNA in biological samples.

Photo-regulation of nucleic acid structure formation using an SNA modified with 8-pyrenylvinyl adenine (^{PV}A)

To achieve a smart molecular system like a molecular robot, a nanomachine, or a molecular device, the ability of the system to respond to stimuli is important. Among potential external stimuli, photo-stimulation is an ideal trigger because it can induce activation of molecules with spatiotemporal control without contaminating the solution.[57,58] For example, hybridization of photo-caged DNA has been activated by irradiation with specific wavelength of light.[40] Reversible photo-control by various strategies considerably extends the flexibility of molecular systems.[34–36,59] Azobenzene-modified DNA, originally developed by our group, can be used for effective photo-control of DNA.[60–63] Recently, XNAs have been used as scaffolds for nanomachines and nanoarchitectures,[64–67] and photo-regulatable XNAs have potential as next-generation materials.

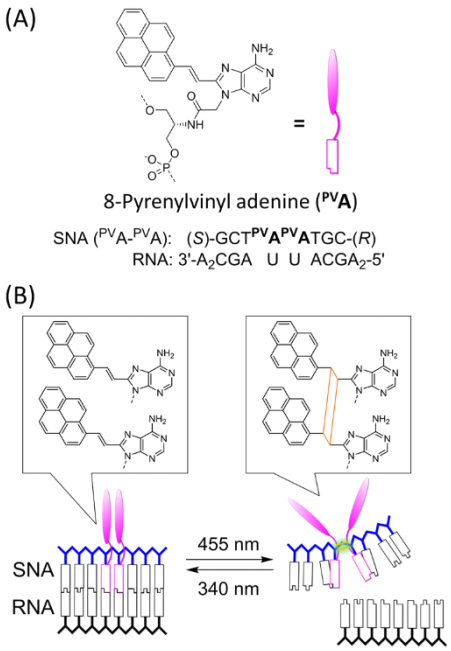

Figure 4. A) Chemical structure of SNA modified with ^{PV}A and sequences of SNA and RNA used in experiments. B) Illustration of reversible photo-regulation of SNA/RNA duplex formation via intrastrand photo-crosslinking of ^{PV}As in the SNA strand. Irradiation with 455 nm blue light induces [2+2] photocycloaddition of the ^{PV}As and dissociation of the duplex, whereas irradiation with 340 nm UV light causes cyclo-reversion and reformation of the duplex.

For DNA photo-regulation, we used base surrogate of azobenzene additionally incorporated into DNA strand via D-threoninol linker (Fig. 1B, upper panel). The *trans*-azobenzene intercalates into base pairs, which stabilizes duplex, while sterically hindered *cis*-azobenzene, induced by UV irradiation, causes destabilization and dissociation of the duplex.[60] However, this system was not suitable for photo-regulation of SNA/RNA duplexes because azobenzene-modified SNA severely destabilized duplexes and caused azobenzene-flipping.[68] To enable photo-regulation of structures formed by SNA, we designed ^{PV}A as photo-responsive adenine analogue and modified an SNA strand with two ^{PV}A residues (Fig. 4A).[68] When an SNA strand containing adjacent ^{PV}A residues is irradiated with blue light (455 nm), [2+2] photocycloaddition between the ^{PV}A residues generates a cyclobutane ring that inhibits duplex formation. Irradiation with 340 nm regenerates monomeric ^{PV}A via a cyclo-reversion reaction allowing duplex formation (Fig. 4B). An 8-mer SNA strand containing two ^{PV}A residues in the center (SNA(^{PV}A-^{PV}A)) designed to be complementary to a model RNA sequence was synthesized via phosphoramidite chemistry. Before irradiation, the T_m of the SNA(^{PV}A-^{PV}A)/RNA duplex was 35.1 °C (Fig. 5A, black line), which was comparable to that of the unmodified 8-mer SNA/RNA duplex (T_m of 35.0 °C). Thus, ^{PV}A pairs with uracil in RNA strand without destabilization of the duplex. After irradiation with 455 nm light at 20 °C, sufficiently lower than T_m, the absorption band due to ^{PV}A at 400-450 nm significantly decreased in intensity, and new bands appeared at 354 and 337 nm (Fig. 5B), clearly indicating that a photo-crosslinking reaction had

occurred between adjacent ^{PV}A residues. A 1000-s irradiation resulted in approximately 80% conversion of the ^{PV}A monomers into a crosslinked dimer, and about 97% of the ^{PV}A monomers were crosslinked after irradiation for 3000 s (Fig. 5B). When this photo-adduct was irradiated with 340 nm light, the cyclo-reversion reaction occurred as indicated by the re-appearance of the absorption band at 400-450 nm and loss of the signals at 354 and 337 nm (Fig. 5C). The reaction half-life was only about 10 s, and 88% of ^{PV}A monomers reached photo stationary state after 600 s of irradiation (Fig. 5C). Although the irradiation to ^{PV}A can cause *cis*-isomerization that should show broad absorption peak at around 376 nm,[69] we only observed photo-crosslinking when there were two adjacent ^{PV}A residues in the SNA strand. In contrast, *cis*-isomerization is observed when a single ^{PV}A residue is incorporated into an SNA strand.[68]

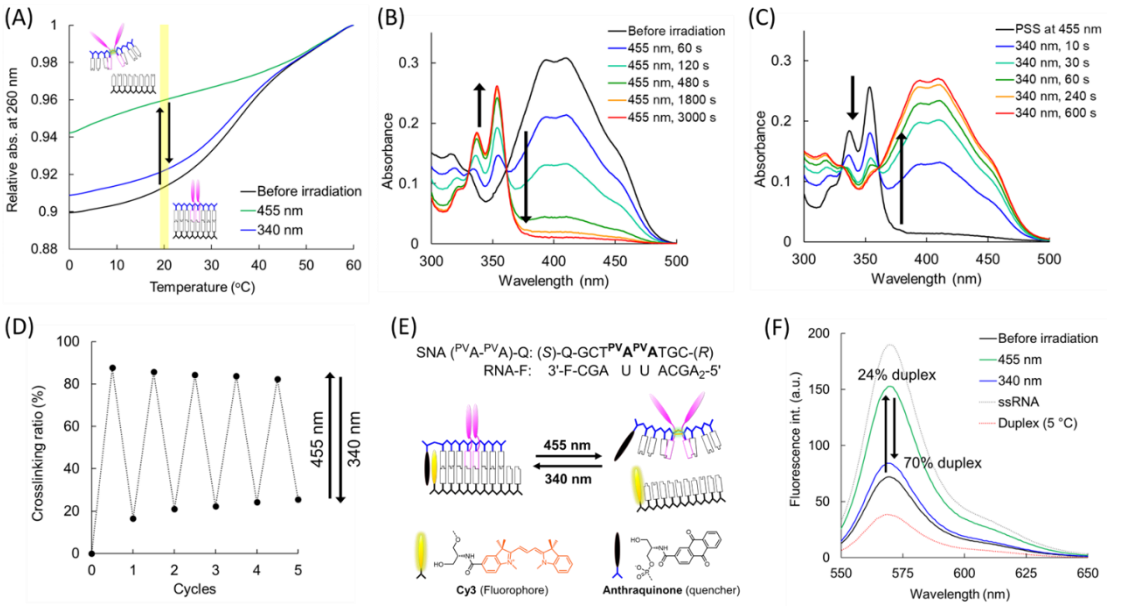

Figure 5. A) Melting profile of SNA(^{PV}A-^{PV}A)/RNA duplex before irradiation (black line), after irradiation with 455 nm light (green line), and after 340 nm light (blue line). B) Absorption spectra of SNA(^{PV}A-^{PV}A)/RNA duplex at indicated times of irradiation with 455 nm light. C) Absorption spectra of photo-stationary state at 455 nm and after irradiation for indicated times with 340 nm light. D) Crosslinking ratios of (^{PV}A-^{PV}A)/RNA after multiple photo-switching cycles. E) Schematic of the fluorescence experiment. Fluorescence from Cy3 tethered to the RNA is quenched by duplex formation with SNA containing anthraquinone. F) Fluorescence spectra of SNA(^{PV}A-^{PV}A)-Q/RNA-F before irradiation (black line), after irradiation with 455 nm (green line), and after irradiation with 340 nm light irradiation (blue line). Ex. = 530 nm. The solution conditions were 100 mM NaCl, 10 mM phosphate buffer (pH 7.0), 5.0 μM oligonucleotide. Adapted with permission from ref. 68 with partial modifications. (Copyright 2019)

Duplex formation was suppressed after irradiation with 455 nm, proving that the SNA(^{PV}A-^{PV}A)/RNA duplex was dissociated via photo-crosslinking of ^{PV}A residues (Fig. 5A, green line). Subsequent irradiation with UV light restored sigmoidal melting (Fig. 5A, blue line), indicating that after cyclo-reversion into ^{PV}A monomers the strand reassociated. This photo-regulation could be repeated by alternating irradiation with 455 nm and with 340 nm light; photobleaching was not significant (Fig. 5D). For direct observation of formation and dissociation of the duplex, an anthraquinone-labeled SNA containing two ^{PV}A residues and a Cy3-labeled RNA were used (Fig. 5E). Before irradiation, the Cy3 emission was quenched by anthraquinone due to duplex formation; about 80% of strands were part of duplexes (Fig. 5F, black line). Irradiation with 455 nm light resulted in recovery of the emission of Cy3, suggesting that about 76% of duplexes were dissociated (Fig. 5F, green line). After irradiation with 340 nm, emission intensity decreased (Fig. 5F, blue line), indicating that about 70% of the duplexes re-formed. Thus, SNA(^{PV}A-^{PV}A)/RNA duplex formation and dissociation can be reversibly regulated at constant temperature. To our knowledge, this is first example of reversible photo-control of duplex formation and dissociation utilizing a photo-crosslinking reaction. The high regulation efficacy using only single pair of ^{PV}As at room temperature and the thermal stability of the photo-adduct are clear advantages over the azobenzene system. Photo-switchable acyclic XNAs thus have potential as photo-regulatable biological tools and nanomachines.

Orthogonal photo-regulation of SNA using ^{PV}A and 8-naphthylvinyl adenine (^{NV}A)

Use of orthogonal photo-regulation that can independently control multiple molecules enables construction of complicated wavelength-selective regulation systems. In the case of DNA, orthogonal photo-regulation by different wavelengths of light has been reported by several groups.[62,70–73] To establish the orthogonal control of two different photo-switching SNA/RNA duplexes, we designed the ^{NV}A base analogue (Fig. 6A).[74] We expected that ^{NV}A would be photo-reactive at shorter wavelength than ^{PV}A due to its smaller conjugation system (Fig. 6B). We prepared an SNA strand containing two adjacent ^{NV}A residues complementary to an RNA target (Fig. 6A). Upon irradiation of the SNA(^{NV}A-^{NV}A)/RNA duplex with 405 nm light, absorbance at around 370 nm decreased considerably (Fig. 6C), indicating formation of a photo-dimer between adjacent ^{NV}A residues via [2+2] photocycloaddition. Almost complete photo-reaction occurred with 2 min of irradiation. A reverse reaction was confirmed by irradiation with 300 nm light; this induced recovery of absorbance around 370 nm (Fig. 6C). The reverse reaction was saturated at about 60% cyclo-reversion after 2 min of irradiation, probably due to overlap of absorption spectra between monomer and dimer forms of ^{NV}A. HPLC analysis also supported these reactions. Further, the photo-dimerization of ^{NV}As significantly reduced thermal stability of the SNA/RNA duplex: the duplex was mostly dissociated upon irradiation with 405 nm light (Fig. 6D, cyan line), whereas 300 nm light induced duplex formation (Fig. 6D, purple line). This indicates that duplex formation and dissociation can be regulated by irradiation with suitable wavelengths of light at 20 °C.

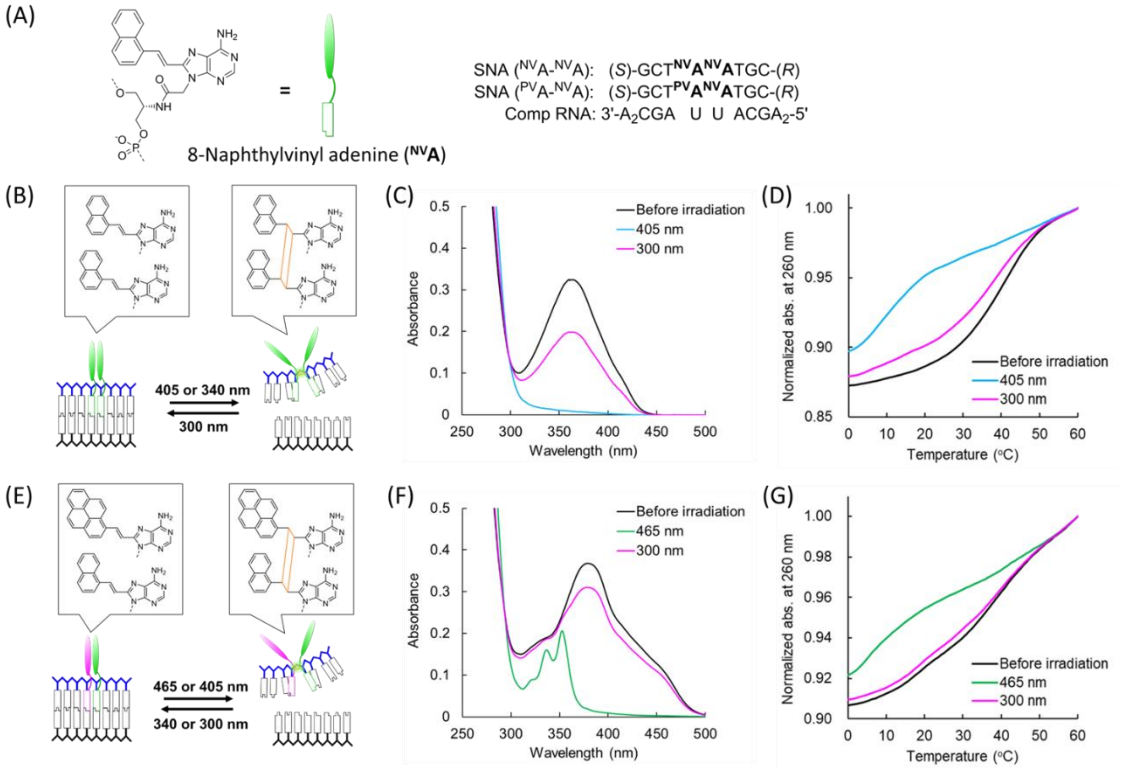

Figure 6. A) Chemical structure of SNA with ^{NV}A and sequences of SNA and RNA. B) Schematic of reversible photo-regulation of SNA(^{NV}A-^{NV}A)/RNA duplex formation. C) Absorption spectra and D) melting profile of SNA(^{NV}A-^{NV}A)/RNA before irradiation (black lines), after irradiation with 405 nm light (cyan lines), and after irradiation with 300 nm light (purple lines). E) Schematic of reversible photo-regulation of SNA(^{PV}A-^{NV}A)/RNA duplex formation. F) Absorption spectra and G) melting profile of SNA(^{PV}A-^{NV}A)/RNA before irradiation (black lines), after irradiation with 465 nm light through a longpass optical filter (450 nm) (green lines), and after irradiation with 300 nm light (purple lines). The solution conditions were 100 mM NaCl, 10 mM phosphate buffer (pH 7.0), 5.0 μM oligonucleotide. Adapted with permission from ref. 74 with partial modifications. (Copyright 2021)

Toward the goal of creating an orthogonal switch, we characterized an SNA containing both ^{PV}A and ^{NV}A (Fig. 6E). We first confirmed that a photo-dimer formed reversibly between adjacent ^{PV}A and ^{NV}A residues (Fig. 6F) and that crosslinking regulated formation of a duplex between SNA(^{PV}A-^{NV}A) and RNA

(Fig. 6G). Heterodimerization of ^{PV}A and ^{NV}A and homodimerization of ^{NV}A and the cyclo-reversions are regulated by different wavelengths of light (Fig. 7A). Formation of the ^{NV}A-^{PV}A hetero pair, but not of the ^{NV}A-^{NV}A pair, is induced by 465 nm irradiation. Both of ^{PV}A-^{NV}A and ^{NV}A-^{NV}A is dimerized by 405 nm irradiation. Cyclo-reversion of the ^{PV}A-^{NV}A dimer results from irradiation with 340 nm light, whereas 300 nm light facilitated cyclo-reversion of both ^{PV}A-^{NV}A and ^{NV}A-^{NV}A. These results indicated that orthogonal control of ^{PV}A-^{NV}A and ^{NV}A-^{NV}A is possible (Figure 7B).

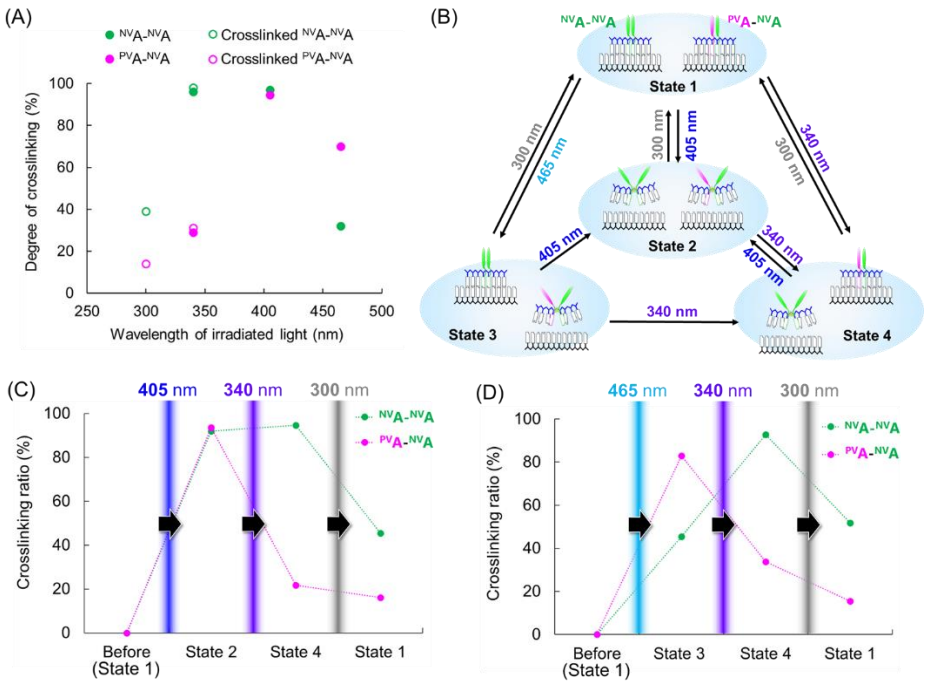

Figure 7. A) Relationship between the percent of crosslinked chromophores of SNA(^{NV}A-^{NV}A)/RNA (green) and SNA(^{PV}A-^{NV}A)/RNA (purple) and irradiation wavelength. Open circles are percent of crosslinked chromophores in SNAs first irradiated with 405 nm light and then with the indicated light of wavelength. Light irradiation was carried out for 20 min at 465 nm through longpass optical filter (450 nm), 60 min at 405 nm, 30 min at 340 nm, and 5 min at 300 nm. B) Illustration of controlled hybridization of two SNA/RNA duplexes. Four possible states of SNA/RNA duplexes can be realized by irradiating with four different wavelengths of light. C, D) Percent crosslinked ^{NV}A/^{NV}A (green) and ^{PV}A/^{NV}A (purple) after irradiation sequentially with C) 405 nm, 340 nm, and 300 nm light and with D) 465 nm, 340 nm, and 300 nm light. The solution conditions were 100 mM NaCl, 10 mM phosphate buffer (pH 7.0), 5.0 μM oligonucleotide. Adapted with permission from ref. 74 with partial modifications. (Copyright 2020)

To experimentally demonstrate orthogonal photo-regulation, crosslinking ratios in a solution of SNA(^{PV}A-^{NV}A), SNA(^{NV}A-^{NV}A), and RNA were analyzed by HPLC. Irradiation with 405 nm light resulted in almost complete photo-cycloaddition of both SNA(^{PV}A-^{NV}A) and SNA(^{NV}A-^{NV}A), subsequent irradiation with 340 nm reversed the crosslink in the SNA(^{PV}A-^{NV}A) strand without disrupting the crosslink in SNA(^{NV}A-^{NV}A), and irradiation with 300 nm light reversed both crosslinks (Fig. 7C). Thus, sequential transitions were induced from State 1 to State 2 to State 4 to State 1 by irradiating with 405 nm, 340 nm, and 300 nm light, respectively (Fig. 7B). Sequential transitions from State 1 to 3 to 4 to 1 were induced by irradiation with 465 nm, 340 nm, and 300 nm light, respectively (Fig. 7D). These results clearly demonstrate selective photo-regulation of the formation and dissociation of two different SNA/RNA duplexes by irradiating with specific wavelengths of light. Intrastrand photo-crosslinking and cyclo-reversion between ^{NV}As was induced by irradiation with shorter wavelengths of light than used for the ^{PV}A-^{NV}A system. Thus, acyclic XNAs carrying photo-responsive nucleobases have a great potential as components of complex, photo-driven molecular systems.

Conclusion and perspective

We have developed valuable biological tools composed of an acyclic XNA with nucleobase modifications. An SNA linear probe carrying three ^{Pe}U residues enabled detection of target RNA through a visually observable change in fluorescent color and intensity. This probe also discriminated an RNA containing a single base mismatch from a fully matched target. Incorporation of ^{PV}A into the SNA strand enabled photo-control of SNA/RNA duplex formation and dissociation. Use of ^{NV}A and ^{PV}A allowed orthogonal control of formation of two different SNA/RNA duplexes; selective generation of four hybridization states were demonstrated. Conjugation of the photo-responsive SNA and the SNA linear prove would realize photo-controllable RNA detection probe that can minimize the suppression of RNA function by control of binding duration, which is suitable for real-time monitoring. This orthogonal system has potential to use as a photo-regulatable molecular system such as a cellular chemical artificial intelligence system.[75]

A critical finding of our work is that nucleobase modifications allow functionalization of acyclic XNA without negative effects on duplex formation. The high flexibility of the acyclic XNA scaffold probably facilitated intrastrand interactions among functional molecules, for example, effective excimer formation between ^{Pe}Us in the single-stranded SNA linear probe and photo-hetero- and homo-dimerizations of ^{PV}A and ^{NV}A in SNA strands. The rigid cyclic ribose of DNA may not allow such effective interactions. Moreover, compared to cyclic XNAs that are complicated to synthesize due to stereochemistry of the cyclic scaffold, the syntheses of acyclic XNAs are facile.

We have also reported other examples of incorporation of unnatural nucleobases into acyclic XNAs. Incorporation of a diaminopurine/thiouracil pair improved hybridization behavior by avoiding self-hybridization of SNA.[76,77] An *a*TNA strand carrying cyanuric acid and aminopyrimidine derivatives form a unique artificial hexaplex structure.[78] We also demonstrated chiral orthogonality between D-*a*TNA and L-*a*TNA: although both D-*a*TNA and L-*a*TNA form highly stable homo-duplexes, hetero-duplex formation between left-handed D-*a*TNA and right-handed L-*a*TNA does not occur.[79] If the ^{NV}A/^{PV}A system, which can be orthogonally photo-controlled, was incorporated into D-*a*TNA and L-*a*TNA, the molecular system could be further expanded due to the addition of chiral orthogonality. Since various functional nucleobases are available, we expect that acyclic XNAs will become widely used in bio-nanotechnology.

CONFLICT OF INTEREST

The authors declare no conflict of interest.

ACKNOWLEDGEMENTS

This work was supported by Grant-in-Aid for Transformative Research Areas “Molecular Cybernetics” JP20H05970 (K. M.), 20H05968 (K. M.), JSPS KAKENHI grants JP20K15399 (K. M.), JP22J01195 (Y. Y.), JP22K14792 (Y. Y.), and JP21H05025 (H. A.). AMED under Grant Number 22am0401007 (H. A.) is also acknowledged.

1. Beaucage SL, Iyer RP. Advances in the Synthesis of Oligonucleotides by the Phosphoramidite Approach. *Tetrahedron* **48**, 2223–2311 (1992).
2. Leumann CJ. DNA analogues: from supramolecular principles to biological properties. *Bioorg. Med. Chem.* **10**, 841–854 (2002).
3. Zhang S, Switzer C, Chaput JC. The Resurgence of Acyclic Nucleic Acids. *Chem. Biodivers.* **7**, 245–258 (2010).
4. Pinheiro VB, Holliger P. The XNA world: progress towards replication and evolution of synthetic genetic polymers. *Curr. Opin. Chem. Biol.* **16**, 245–252 (2012).
5. Krishnamurthy R. On the Emergence of RNA. *Isr. J. Chem.* **55**, 837–850 (2015).
6. Chaput JC, Herdewijn P. What Is XNA? *Angew. Chem. Int. Ed.* **58**, 11570–11572 (2019).
7. Murayama K, Asanuma H. Design and Hybridization Properties of Acyclic Xeno Nucleic Acid Oligomers. *ChemBioChem* **22**, 2507–2515 (2021).
8. Asanuma H, Kamiya Y, Kashida H, Murayama K. Xeno nucleic acids (XNAs) having non-ribose scaffolds with unique supramolecular properties. *Chem. Commun.* **28**, 3993 (2022).
9. Hövelmann F, Seitz O. DNA Stains as Surrogate Nucleobases in Fluorogenic Hybridization Probes. *Acc. Chem. Res.* **49**, 714–723 (2016).
10. Samanta D, Ebrahimi SB, Mirkin CA. Nucleic-Acid Structures as Intracellular Probes for Live Cells. *Adv. Mater.* **32**, 1901743 (2020).
11. Vilaivan T. Fluorogenic PNA probes. *Beilstein J. Org. Chem.* **14**, 253–281 (2018).
12. Obad S, dos Santos CO, Petri A, Heidenblad M, Broom O, Ruse C, Fu C, Lindow M, Stenvang J, Straarup EM, Hansen HF, Koch T, Pappin D, Hannon GJ, Kauppinen S. Silencing of microRNA families by seed-targeting tiny LNAs. *Nat. Genet.* **43**, 371–378 (2011).
13. Rooij E, Kauppinen S. Development of microRNA therapeutics is coming of age. *EMBO Mol. Med.* **6**, 851–864 (2014).
14. Le BT, Chen S, Abramov M, Herdewijn P, Veedu RN. Evaluation of anhydrohexitol nucleic acid, cyclohexenyl nucleic acid and D-altritol nucleic acid-modified 2′-O-methyl RNA mixmer antisense oligonucleotides for exon skipping in vitro. *Chem. Commun.* **52**, 13467–13470 (2016).
15. McClorey G, Moulton HM, Iversen PL, Fletcher S, Wilton SD. Antisense oligonucleotide-induced exon skipping restores dystrophin expression in vitro in a canine model of DMD. *Gene Ther.* **13**, 1373–1381 (2006).
16. Laursen MB, Pakula MM, Gao S, Fluiter K, Mook OR, Baas F, Langklær N, Wengel SL, Wengel J, Kjems J, Bramsen JB. Utilization of unlocked nucleic acid (UNA) to enhance siRNA performance in vitro and in vivo. *Mol. Biosyst.* **6**, 862 (2010).
17. Takahashi M, Nagai C, Hatakeyama H, Minakawa N, Harashima H, Matsuda A. Intracellular stability of 2′-OMe-4′-thioribonucleoside modified siRNA leads to long-term RNAi effect. *Nucleic Acids Res.* **40**, 5787–5793 (2012).
18. Schlegel MK, Foster DJ, Kel'in AV, Zlatev I, Bisbe A, Jayaraman M, Lackey JG, Rajeev KG, Charissé K, Harp J, Pallan PS, Maier MA, Egli M, Manoharan M. Chirality Dependent Potency Enhancement and Structural Impact of Glycol Nucleic Acid Modification on siRNA. *J. Am. Chem. Soc.* **139**, 8537–8546 (2017).
19. Khvorova A, Watts JK. The chemical evolution of oligonucleotide therapies of clinical utility. *Nat. Biotechnol.* **35**, 238–248 (2017).
20. Yu H, Zhang S, Chaput JC. Darwinian evolution of an alternative genetic system provides support for TNA as an RNA progenitor. *Nat. Chem.* **4**, 183–187 (2012).
21. Taylor AI, Pinheiro VB, Smola MJ, Morgunov AS, Peak-Chew S, Cozens C, Weeks KM, Herdewijn P, Holliger P. Catalysts from synthetic genetic polymers. *Nature* **518**, 427–430 (2015).
22. Eremeeva E, Fikatas A, Margamuljana L, Abramov M, Schols D, Groaz E, Herdewijn P. Highly stable hexitol based XNA aptamers targeting the vascular endothelial growth factor. *Nucleic Acids Res.* **47**, 4927–4939 (2019).
23. Hoshino H, Kasahara Y, Kuwahara M, Obika S. DNA Polymerase Variants with High Processivity and Accuracy for Encoding and Decoding Locked Nucleic Acid Sequences. *J. Am. Chem. Soc.* **142**, 21530–21537 (2020).
24. Asanuma H, Toda T, Murayama K, Liang X, Kashida H. Unexpectedly Stable Artificial Duplex from Flexible Acyclic Threoninol. *J. Am. Chem. Soc.* **132**, 14702–14703 (2010).
25. Murayama K, Kashida H, Asanuma H. Acyclic L-threoninol nucleic acid (L-aTNA) with suitable structural rigidity cross-pairs with DNA and RNA. *Chem. Commun.* **51**, 6500–6503 (2015).
26. Murayama K, Kashida H, Asanuma H. Methyl group configuration on acyclic threoninol nucleic acids (aTNAs) impacts supramolecular properties. *Org. Biomol. Chem.* **20**, 4115–4122 (2022).
27. Kashida H, Murayama K, Toda T, Asanuma H. Control of the Chirality and Helicity of Oligomers of Serinol Nucleic Acid (SNA) by Sequence Design. *Angew. Chem. Int. Ed.* **50**, 1285–1288 (2011).
28. Murayama K, Kamiya Y, Kashida H, Asanuma H. Ultrasensitive Molecular Beacon Designed with Totally Serinol Nucleic Acid (SNA) for Monitoring mRNA in Cells. *ChemBioChem* **16**, 1298–1301 (2015).
29. Le BT, Murayama K, Shabanpoor F, Asanuma H, Veedu RN. Antisense oligonucleotide modified with serinol nucleic acid (SNA) induces exon skipping in mdx myotubes. *RSC Adv.* **7**, 34049–34052 (2017).
30. Asanuma H, Murayama K, Kamiya Y, Kashida H. The DNA Duplex as an Aqueous One-Dimensional Soft Crystal Scaffold for Photochemistry. *Bull. Chem. Soc. Jpn.* **91**, 1739–1748 (2018).
31. Asanuma H, Murayama K, Kamiya Y, Kashida H. Design of photofunctional oligonucleotides by copolymerization of natural nucleobases with base surrogates prepared from acyclic scaffolds. *Polym. J.* **49**, 279–289 (2017).

32. Abdelhady AM, Onizuka K, Ishida K, Yajima S, Mano E, Nagatsugi F. Rapid Alkene–Alkene Photo-Cross-Linking on the Base-Flipping-Out Field in Duplex DNA. *J. Org. Chem.* **87**, 2267–2276 (2022).
33. Morihiro K, Kodama T, Waki R, Obika S. Light-triggered strand exchange reaction using the change in the hydrogen bonding pattern of a nucleobase analogue. *Chem. Sci.* **5**, 744–750 (2014).
34. Barrois S. Wagenknecht HA. Diarylethene-modified nucleotides for switching optical properties in DNA. *Beilstein J. Org. Chem.* **8**, 905–914 (2012).
35. Cahová H, Jäschke A. Nucleoside-Based Diarylethene Photoswitches and Their Facile Incorporation into Photoswitchable DNA. *Angew. Chem. Int. Ed.* **52**, 3186–3190 (2013).
36. Ogasawara S, Maeda M. Straightforward and Reversible Photoregulation of Hybridization by Using a Photochromic Nucleoside. *Angew. Chem. Int. Ed.* **47**, 8839–8842 (2008).
37. Wada T, Minamimoto N, Inaki Y, Inoue Y. Peptide Ribonucleic Acids (PRNA). 2. A Novel Strategy for Active Control of DNA Recognition through Borate Ester Formation. *J. Am. Chem. Soc.* **122**, 6900–6910 (2000).
38. Ohkubo A, Kasuya R, Miyata K, Tsunoda H, Seio K, Sekine M. New thermolytic carbamoyl groups for the protection of nucleobases. *Org. Biomol. Chem.* **7**, 687 (2009).
39. Scharf P, Müller J. Nucleic Acids With Metal-Mediated Base Pairs and Their Applications. *Chempluschem* **78**, 20–34 (2013).
40. Liu Q, Deiters A. Optochemical Control of Deoxyoligonucleotide Function via a Nucleobase-Caging Approach. *Acc. Chem. Res.* **47**, 45–55 (2014).
41. Dietzsch J, Bialas D, Bandorf J, Würthner F, Höbartner C. Tuning Exciton Coupling of Merocyanine Nucleoside Dimers by RNA, DNA and GNA Double Helix Conformations. *Angew. Chem. Int. Ed.* **61**, (2022).
42. Seo YJ, Rhee H, Joo T, Kim BH. Self-Duplex Formation of an A Py -Substituted Oligodeoxyadenylate and Its Unique Fluorescence. *J. Am. Chem. Soc.* **129**, 5244–5247 (2007).
43. Okamoto A, Kanatani K, Saito I. Pyrene-Labeled Base-Discriminating Fluorescent DNA Probes for Homogeneous SNP Typing. *J. Am. Chem. Soc.* **126**, 4820–4827 (2004).
44. Skorobogatyi MV, Malakhov AD, Pchelintseva AA, Turban AA, Bondarev SL, Korshun VA. Fluorescent 5-Alkynyl-2′-Deoxyuridines: High Emission Efficiency of a Conjugated Perylene Nucleoside in a DNA Duplex. *ChemBioChem* **7**, 810–816 (2006).
45. Börjesson K, Preus S, El-Sagheer AH, Brown T, Albinsson B, Wilhelmsson LM. Nucleic Acid Base Analog FRET-Pair Facilitating Detailed Structural Measurements in Nucleic Acid Containing Systems. *J. Am. Chem. Soc.* **131**, 4288–4293 (2009).
46. Han JH, Yamamoto S, Park S, Sugiyama H. Development of a Vivid FRET System Based on a Highly Emissive dG-dC Analogue Pair. *Chem. - A Eur. J.* **23**, 7607–7613 (2017).
47. Okamura H, Trinh GH, Dong Z, Masaki Y, Seio K, Nagatsugi F. Selective and stable base pairing by alkynylated nucleosides featuring a spatially-separated recognition interface. *Nucleic Acids Res.* **50**, 3042–3055 (2022).
48. Morihiro K, Moriyama Y, Nemoto Y, Osumi H, Okamoto A. anti–syn Unnatural Base Pair Enables Alphabet-Expanded DNA Self-Assembly. *J. Am. Chem. Soc.* **143**, 14207–14217 (2021).
49. Takezawa Y, Suzuki A, Nakaya M, Nishiyama K, Shionoya M. Metal-Dependent DNA Base Pairing of 5-Carboxyuracil with Itself and All Four Canonical Nucleobases. *J. Am. Chem. Soc.* **142**, 21640–21644 (2020).
50. Kimoto M, Kawai R, Mitsui T, Yokoyama S, Hirao I. An unnatural base pair system for efficient PCR amplification and functionalization of DNA molecules. *Nucleic Acids Res.* **37**, e14–e14 (2009).
51. Malyshev DA, Seo YJ, Ordoukhanian P, Romesberg FE. PCR with an Expanded Genetic Alphabet. *J. Am. Chem. Soc.* **131**, 14620–14621 (2009).
52. Kaul C, Müller M, Wagner M, Schneider S, Carell T. Reversible bond formation enables the replication and amplification of a crosslinking salen complex as an orthogonal base pair. *Nat. Chem.* **3**, 794–800 (2011).
53. St Johnston D. Moving messages: the intracellular localization of mRNAs. *Nat. Rev. Mol. Cell Biol.* **6**, 363–375 (2005).
54. Bratu DP, Cha BJ, Mhlanga MM, Kramer FR, Tyagi S. Visualizing the distribution and transport of mRNAs in living cells. *Proc. Natl. Acad. Sci.* **100**, 13308–13313 (2003).
55. Asanuma H, Akahane M, Kondo N, Osawa T, Kato T, Kashida H. Quencher-free linear probe with multiple fluorophores on an acyclic scaffold. *Chem. Sci.* **3**, 3165 (2012).
56. Murayama K, Asanuma H. A Quencher‐Free Linear Probe from Serinol Nucleic Acid with a Fluorescent Uracil Analogue. *ChemBioChem* **21**, 120–128 (2020).
57. Brieke C, Rohrbach F, Gottschalk A, Mayer G, Heckel A. Light‐Controlled Tools. *Angew. Chem. Int. Ed.* **51**, 8446–8476 (2012).
58. Lubbe AS, Szymanski W, Feringa BL. Recent developments in reversible photoregulation of oligonucleotide structure and function. *Chem. Soc. Rev.* **46**, 1052–1079 (2017).
59. Yoshimura Y, Fujimoto K. Ultrafast Reversible Photo-Cross-Linking Reaction: Toward in Situ DNA Manipulation. *Org. Lett.* **10**, 3227–3230 (2008).
60. Asanuma H, Liang X, Nishioka H, Matsunaga D, Liu M, Komiyama M. Synthesis of azobenzene-tethered DNA for reversible photo-regulation of DNA functions: hybridization and transcription. *Nat. Protoc.* **2**, 203–212 (2007).
61. Goldau T, Murayama K, Brieke C, Steinwand S, Mondal P, Biswas M, Burghardt I, Wachtveitl J, Asanuma H, Heckel A. Reversible Photoswitching of RNA Hybridization at Room Temperature with an Azobenzene C -Nucleoside. *Chem. - A Eur. J.* **21**, 2845–2854 (2015).
62. Škugor M, Valero J, Murayama K, Centola M, Asanuma H, Famulok M. Orthogonally Photocontrolled Non‐Autonomous DNA Walker. *Angew. Chem. Int. Ed.* **58**, 6948–6951 (2019).

63. Kamiya Y, Asanuma H. Light-Driven DNA Nanomachine with a Photoresponsive Molecular Engine. *Acc. Chem. Res.* **47**, 1663–1672 (2014).
64. Wenge U, Wengel J, Wagenknecht HA. Photoinduced Reductive Electron Transfer in LNA:DNA Hybrids: A Compromise between Conformation and Base Stacking. *Angew. Chem. Int. Ed.* **51**, 10026–10029 (2012).
65. Zhang RS, McCullum EO, Chaput JC. Synthesis of Two Mirror Image 4-Helix Junctions Derived from Glycerol Nucleic Acid. *J. Am. Chem. Soc.* **130**, 5846–5847 (2008).
66. Hsieh WC, Martinez GR, Wang A, Wu SF, Chamdia R, Ly DH. Stereochemical conversion of nucleic acid circuits via strand displacement. *Commun. Chem.* **1**, 89 (2018).
67. Kim KT, Angerani S, Winssinger NA. minimal hybridization chain reaction (HCR) system using peptide nucleic acids. *Chem. Sci.* **12**, 8218–8223 (2021).
68. Murayama K, Yamano Y, Asanuma H. 8-Pyrenylvinyl Adenine Controls Reversible Duplex Formation between Serinol Nucleic Acid and RNA by [2 + 2] Photocycloaddition. *J. Am. Chem. Soc.* **141**, 9485–9489 (2019).
69. Kovalenko NP, Abdukadyrov AT, Gerko VI, Alfimov MV. Luminescent and photochemical behaviour of diarylethylenes with 3-pyrenyl substituents. *J. Photochem.* **12**, 59–65 (1980).
70. Rodrigues-Correia A, Weyel XMM, Heckel A. Four Levels of Wavelength-Selective Uncaging for Oligonucleotides. *Org. Lett.* **15**, 5500–5503 (2013).
71. Fujimoto K, Sasago S, Mihara J, Nakamura S. DNA Photo-cross-linking Using Pyranocarbazole and Visible Light. *Org. Lett.* **20**, 2802–2805 (2018).
72. Nishioka H, Liang X, Kato T, Asanuma H. A Photon-Fueled DNA Nanodevice that Contains Two Different Photoswitches. *Angew. Chem. Int. Ed.* **51**, 1165–1168 (2012).
73. Haydell MW, Centola M, Adam V, Valero J, Famulok M. Temporal and Reversible Control of a DNAzyme by Orthogonal Photoswitching. *J. Am. Chem. Soc.* **140**, 16868–16872 (2018).
74. Yamano Y, Murayama K, Asanuma H. Dual Crosslinking Photo‐Switches for Orthogonal Photo‐Control of Hybridization Between Serinol Nucleic Acid and RNA. *Chem. – A Eur. J.* **27**, 4599–4604 (2021).
75. Murata S, Toyota T, Nomura SM, Nakakuki T, Kuzuya A. Molecular Cybernetics: Challenges toward Cellular Chemical Artificial Intelligence. *Adv. Funct. Mater.* **32**, 2201866 (2022).
76. Kamiya Y, Donoshita Y, Kamimoto H, Murayama K, Ariyoshi J, Asanuma, H. Introduction of 2,6-Diaminopurines into Serinol Nucleic Acid Improves Anti-miRNA Performance. *ChemBioChem* **18**, 1917–1922 (2017).
77. Sato F, Kamiya Y, Asanuma H. Syntheses of Base-Labile Pseudo-Complementary SNA and L-*a*TNA Phosphoramidite Monomers. *J. Org. Chem.* (2023) doi:10.1021/acs.joc.2c01911.
78. Kashida H, Hattori Y, Tazoe K, Inoue T, Nishikawa K, Ishii K, Uchiyama S, Yamashita H, Abe M, Kamiya Y, Asanuma H. Bifacial Nucleobases for Hexaplex Formation in Aqueous Solution. *J. Am. Chem. Soc.* **140**, 8456–8462 (2018).
79. Chen Y, Nagao R, Murayama K, Asanuma H. Orthogonal Amplification Circuits Composed of Acyclic Nucleic Acids Enable RNA Detection. *J. Am. Chem. Soc.* **144**, 5887–5892 (2022).

Graphical Abstract

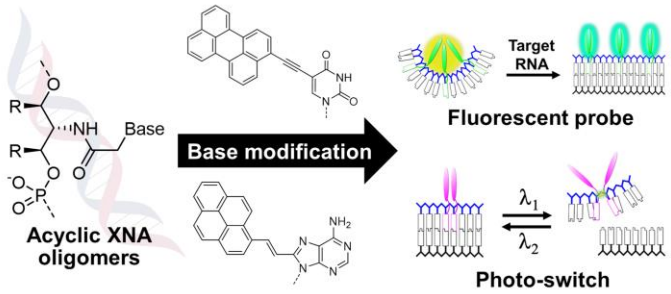

Nucleobase modification on acyclic XNA oligomers achieved functionalization as novel fluorescent probe and photo-switch system.